IOP Conf. Series: Materials Science and Engineering **382** (2018) 022082 doi:10.1088/1757-899X/382/2/022082

Experimental Study on Density and Pore Defect of Cobalt-chromium Alloy Manufactured by Selective Laser Melting

C An[1,2], J S Zhang[1], Y M Zhang [2,3,5], D X Lv [2,3] and L Ruan [4]

[1] School of Mechatronic Engineering and Automation, Shanghai University, Shanghai 200070, China;

[2] Institute of Material Technology and engineering, CAS, Ningbo 315200, China;

[3] Key Laboratory of Zhejiang Province on Additive Manufacturing Materials Technology, Ningbo 315200, China;

[4] Ningbo Runyes Medical Instrument Co. Ltd, Ningbo 315200, China

zhangyuanming@nimte.ac.cn

Abstract. In this paper, an orthogonal experiment was designed to fabricate the selective laser melting cobalt-chromium alloy samples. The influence rules of varying process parameters on the samples' relative density was studied. The type and distribution of pore defect in the forming part were observed, and the pore formation mechanism was analysed, then porosity prevention measures were proposed. Experimental results show that: powder thickness affects the density of SLM forming parts most. Pore defect is one of the most important defects that affect the density. Pore defect can be divided into two types: keyhole and gas hole pore. The former is larger and irregular, caused by the underlying part of powder not melting completely due to the spheroidization effect and volume shrinkage effect of uneven powder thickness. The latter is smaller and round, mainly caused by the bubbles of nitrogen and vaporization of low melting point constituents discharging not timely. Reducing the thickness of the powder can effectively eliminate keyhole pore defects, and pre-heating the substrate before forming can reduce the occurrence of gas hole pore defects.

1. Introduction

Currently selective laser melting (SLM) technology has been one of the fastest growing additive manufacturing technologies available. It is based on the dispersion-deposition principle, and fabricates high-performance metal parts directly by layered manufacturing methods. Application of metal parts printing is becoming more and more valuable and has been the current research hotspots globally [1-2]. The demand for personalized medical products is increasing day by day. Compared with the traditional manufacturing technology, SLM technology can not only meet the cost reduction requirements, but also meet the needs of patients with personalized differences. Especially in terms of implants, it can achieve better adaptability [3-4]. Because of high strength, excellent fatigue resistance, good biocompatibility and high metal-ceramic bonding strength, cobalt-chromium alloy has received widespread attention, and is commonly used as medical materials [5-8]. Relative density is one of the most important properties to evaluate the quality of SLM forming parts. However, pore defect is an crucial type of defect that will reduce the density of forming parts. Low density affects the mechanical properties of the cobalt-chromium alloy SLM forming parts such as tensile strength, hardness and so on [9-10]. Therefore, study on the influence law on the density of cobalt-chromium alloy SLM

forming parts, pore defects formation mechanism and measures to reduce the porosity is of great significance to improve the synthesized mechanical properties of SLM forming parts.

A lot of studies on density and pore defect of SLM forming parts have been performed at home and abroad. Santos et al. [11] found that adjusting the powder layer thickness and scanning space can increase the density of parts. Lu et al. [12] obtained dense CoCrW alloy by line and by film scanning strategy. Aboulkhair et al. [13] studied the AlSi10Mg alloy SLM forming process, and two types of defect were found on either side of the optimal scanning speed range. One is metallurgical pore at low scan speeds, and the other is the keyhole pore at high scan speeds. Metallurgical pore was also called hydrogen porosity, and its shape is smaller and spherical, which is due to the retention of gas generated from the melt pool. Keyhole pore is larger in size and irregular in shape, which is caused by keyhole instability due to laser-material interaction or Inadequate powder melting. Monroy et al. [14] regulate internal porosity by adjusting energy input by regulating process parameters in the CoCrMo alloy SLM forming process. The author considered that a large number of randomly distributed circular pores mainly come from gas retention, and such defect will promote if the melting pool staying high temperature for a bit long time. Smaller circular pores are caused by gas retention in the melting pool, however, there are different opinions on gas source among scholars. The literature [13] mentions that most authors believe that the gas comes from the interior of the powder particles or from the initial gas retained by the powder bed particles (Ar or N_2). Gong et al. [15] studied the SLM pore defect morphology and classification of titanium alloy with statistical method, and argued that it is related to the low melting point gasification during laser-powder interaction when the melting pool is extremely unstable, gas generated in the bottom and can't escape because of rapid solidification, then formed a large number of pores.

In this study, an orthogonal experiment was used to prepare the selective laser melting cobalt-chromium alloy parts. Laser power, scanning speed, powder thickness and scanning distance four process parameters was selected as the experimental variables. The influence rules of the above four process parameters on the density of SLM forming parts was explored. Then the morphology and distribution of pore defect were observed and analyzed. At last its generation mechanism and defect eliminating method were proposed.

2. Experiment

2.1. Experimental equipment

In the experiment, the selective laser melting equipment is developed by Ningbo Institute of Materials Technology and Engineering, Chinese Academy of Sciences independently. The equipment schematic is shown in Figure 1.

The SLM equipment is equipped with an IPG continuous fiber laser rated at 200W with wavelength of 1064nm and spot diameter of about 0.1mm. Its optical system includes beam expander, f-θ lens et al. and its scanning system includes X/Y axis scanning galvanometer, galvanometer motion control card et al. The maximum scanning speed is up to 7m/s and maximum working size of forming cavity is φ100mm×300mm. Meanwhile the device is also equipped with gas circulation protection system, which can protect the part from being oxidized during the forming process.

2.2. Experimental Materials

In order to meet the forming process requirements, aerosol spherical powder with lower oxygen content was used in the experiment. Oerlikon cobalt-chromium alloy powder was chosen as the experimental material, whose composition is in full compliance with medical standards, and 90% of the powder has a particle size of 49μm or less. The powder SEM micro-topography was shown in Figure 2, and the specific composition of the ingredients was shown in Table 1.

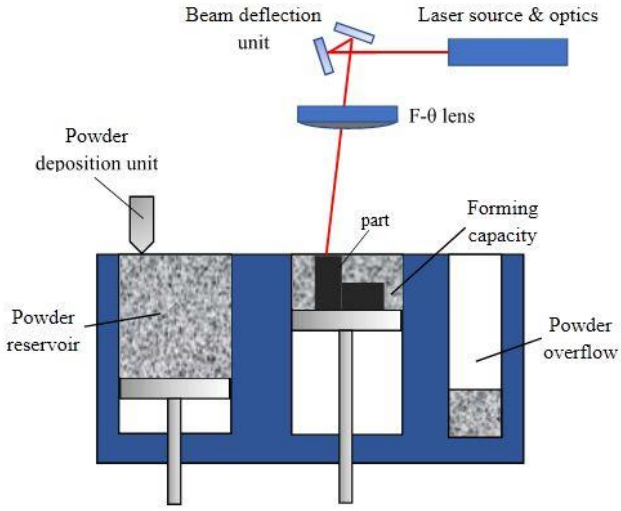

Figure 1. SLM equipment schematic

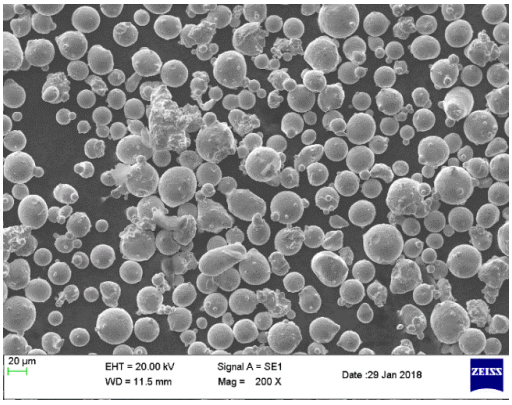

Figure 2. Cobalt-chromium alloy powder SEM morphology

Table 1. Cobalt-chromium alloy powder chemical element content

chemical element	Co	Cr	Mo	C	Other
Percentage (%)	Balance	29	6	<0.06	<0.1

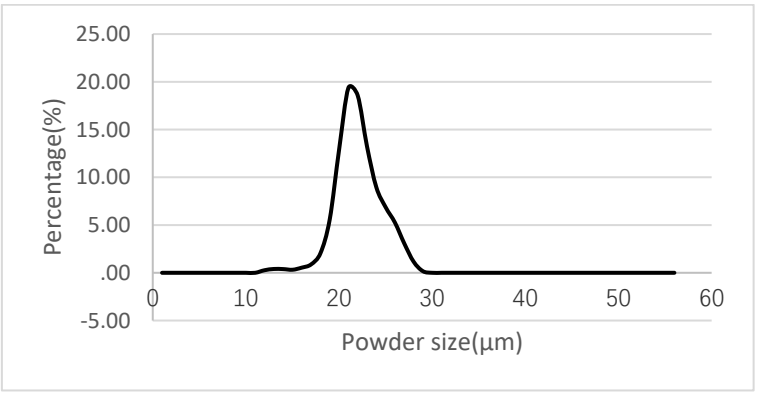

Figure 3. Powder particle size distribution

2.3. Experiment procedure

As follows are the experiment procedures:

- Convert 3D CAD model files to STL format files, then import it into Magics software to slice and fill the path. Scanning strategy is shown in Figure 4. Get a JOB file that can be printed, and then the JOB file is loaded into the operating software in the industrial computer.
- Control the scraper inside the forming cavity to lay a layer of cobalt chromium alloy powder on the substrate, then preheat the powder to about 60°C.
- The laser scans the powder to form a molten pool then quickly solidify.
- After one layer is scanned off, the forming piston drops down a layer of height, and the powder feeding piston rises more than one layer of height. Then the scraper lays the powder on the substrate with left and right movement. Next, the laser beam scans powder cyclically till the final formation of three-dimensional parts finishes.
- Remove excess powder, then get the part after removing the substrate from the piston.

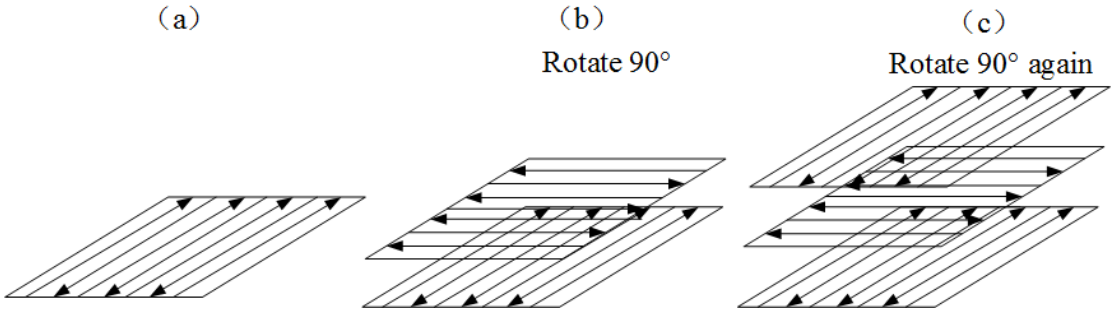

Figure 4. Scanning strategy diagram

3. Results and discussion

3.1. Influence rules analysis of process parameters on density

The experiment studied the influence rules of laser power, scanning speed, powder thickness, scanning distance four process parameters on the SLM forming cobalt-chromium alloy density and morphology of pore defect, and orthogonal experiment of four factors and three levels was designed The experimental results are shown in Table 2. And the range analysis results are shown in Table 3.

Table 2. Orthogonal experimental results

No.	Laser power (W)	Scanning speed (mms^{-1})	Powder thickness (mm)	Scanning distance (mm)	Relative density (%)
1	130	300	0.03	0.04	95.13
2	130	400	0.05	0.06	94.70
3	130	500	0.07	0.08	95.24
4	150	300	0.07	0.06	94.09
5	150	400	0.03	0.08	95.77
6	150	500	0.05	0.04	95.04
7	170	300	0.05	0.08	95.97
8	170	400	0.07	0.04	94.64
9	170	500	0.03	0.06	96.59

Table 3. Range results of density

Range results	Laser power	Scanning speed	Powder thickness	Scanning distance
Relative density	0.77	0.58	1.17	0.72

As can be seen from Table 3, the descending order of the factors that affect the density are: powder thickness> laser power> scanning distance> scanning speed. Therefore, powder thickness is the most important factor affecting the density of SLM forming parts. The highest density of SLM forming parts at the process parameters of P=170 W, V=500mm/s, h=0.03mm, d=0.08mm is up to 97.05%.

According to the result of orthogonal experiment, the influence curve of each factor on the density is shown in Fig.5.

- When the laser power is smaller, the powder absorbs less heat, and the viscosity of the melted is higher. Spheroidization occurs because the melting pool has a larger infiltration angle, which causes forming layer surface uneven, then affects the pavement quality of next powder layer. As a result of being worse layer by layer, the density of forming parts is smaller. As the laser power increases, heat radiation received by the powder increases, and the temperature is constantly rising, so the amount of powder melted increases, and the melting pool becomes

wider and deeper. Thus the adjacent melting pools bond more closely. As a consequence, the density of forming parts increases.

- When the scanning speed is too small, laser irradiates powder bed longer, and powder absorbs too much heat per unit of time, which causes over burning and rough forming surface, which affects the pavement quality of next powder layer, therefore the density of forming parts decreases as pavement quality being worse layer by layer. As the scanning speed increases, heat radiation received by the powder decreases, resulting in that width of molten pool gets moderate. The adjacent melting lines bond more closely, so the density increases. However, when the scanning speed is too large, intermittent melting causes spheroidization effect. Consequently, the density also decreases.
- When the powder thickness is smaller, the laser can fully melt the powder layer, and the molten pool has a smaller infiltration angle, leading to more flat forming surface, resulting in high-density forming part. As the powder thickness increases, due to the limited depth of laser melting, part of the underlying powder can't be completely melted. Meanwhile because of the balling effect caused by surface tension, the forming layer surface is quite rough. After cumulative deterioration layer by layer, internal porosity of the part increases, resulting in lower density.
- When the scanning distance is too small, the overlap rate of adjacent melting lines is too large, and the melted lines are reheated and melted again, even accompanied with vaporization, causing over burning. The rough forming surface affects the pavement quality of next layer of powder, which resulting in lower density with cumulative deterioration layer by layer. As the scanning distance increases, the overlap rate between scan lines becomes moderate, causing density of forming parts increasing. As the scanning distance continues to increase, scanning lines transit from overlapping to non-overlapping. The forming surface becomes rough because of too large adjacent melting gap, which affects the uniformity of next powder thickness, thus part of the underlying powder can't be completely melted, resulting in reduced density.

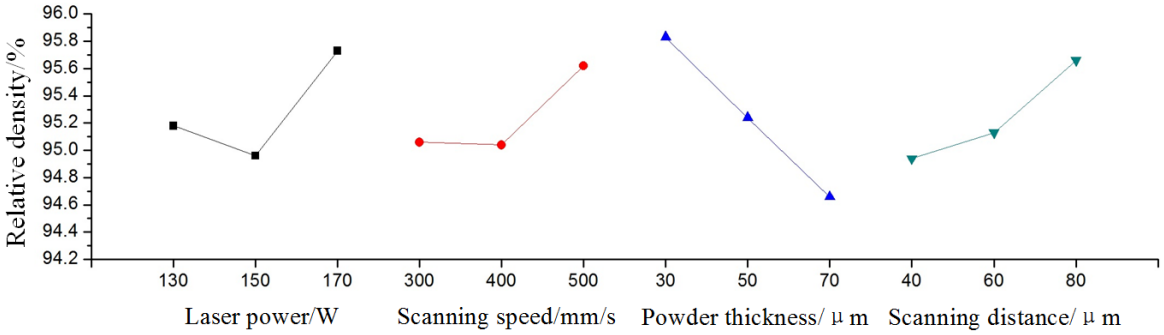

Figure 5. Influence curve of four factors on the relative density

3.2. Pore defect morphology analysis

According to the orthogonal experiment results, the 4th group, the 6th group, the 9th group of forming samples were taken to inlay, grind and polish. The internal morphology of the forming parts was observed under a scanning electron microscope, as shown in Figure 6.

As can be seen from Table 3, the density of the 4th group, the 6th group and the 9th group were 94.09%, 95.04% and 96.59%. The amount of pore in Fig. 6 (a), (b) and (c) decreases in order, and the size of pore decreases in turn. It is concluded that the amount and size of pore have a direct impact on the density of SLM forming parts, and higher density samples corresponds with less internal pores and smaller size.

As can be seen from Figure 6, there are pores of larger size (between tens of microns and hundreds of microns) and irregular shape, named keyhole defect [13]. In contrast, there are also pores of smaller

size (Between tens of nanometers and a few microns) and nearly round shape, as can be seen in figure 7a. Figure 7b shows further magnifying microporous morphology.

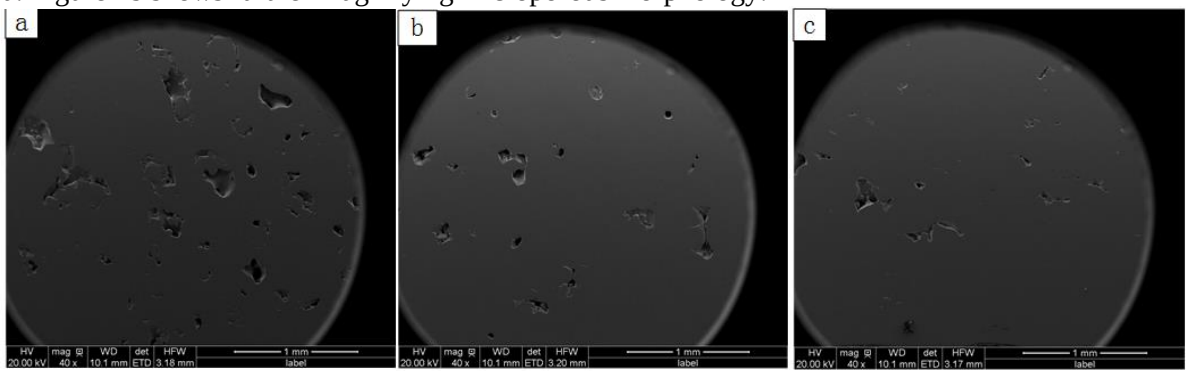

Figure 6. SEM images of SLM forming parts internal morphology

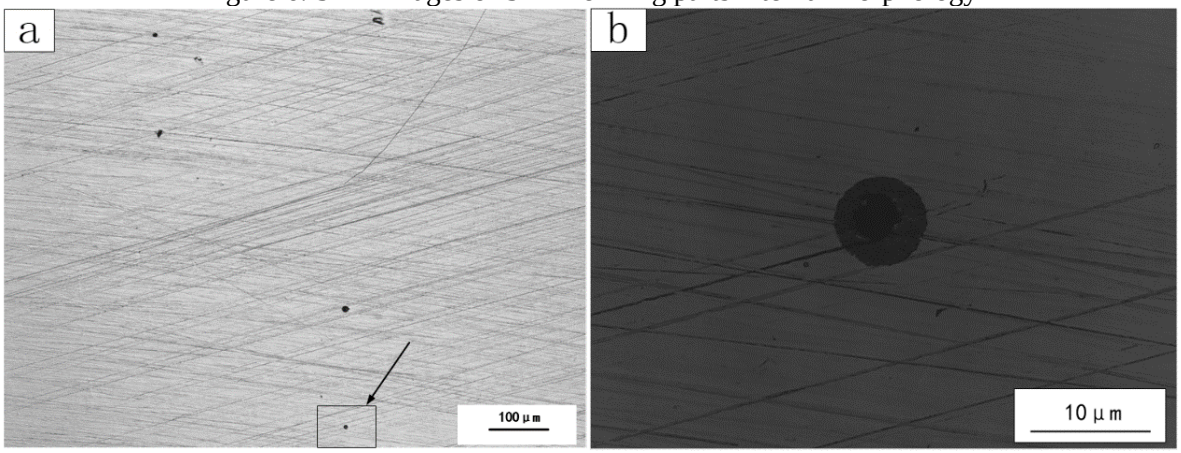

Figure 7. Optical images of SLM forming parts internal round pores morphology

3.3. Pore defect formation mechanism analysis

As follows are the main forming reasons of pore defect analyzed according to its shape, size and distribution above.

3.3.1. Keyhole pore defect formation mechanism analysis

Cobalt-chromium alloy SLM forming is an unstable process controlled by non-uniform temperature gradient, surface tension gradient, thermal capillary action and melt bubble movement. These mutually coupled non-steady-state processes will lead to uncontrollable melt flow behavior, and the formation of pore defect is directly related to the spheroidization effect [16]. With high-energy laser beam rapidly scans line by line, the melt will form a cylindrical trajectory in the laser scanning direction. In order to reduce the surface area and the liquid surface energy, it has a tendency to split into a row of spherical surface, known as the "spheroidization effect" [17]. As shown in Figure 8, θ represents infiltration angle, and S represents solid substrate, and V represents gas environment, and L represents a metal droplet, $F_{S,L}$ represents the solid-liquid interface tension, $F_{V,L}$ represents gas-liquid interface tension, $F_{S,V}$ represents solid-gas interface tension. The thermodynamic equilibrium equation is

$$F_{S,L} + F_{V,L}\cos\theta = F_{S,V} \tag{1}$$

So, infiltration angle

$$\theta = \arccos[(F_{S,V} - F_{S,L})/F_{V,L}] \tag{2}$$

It can be seen from the above formula that the magnitude of the infiltration angle θ reflects the wettability of the liquid phase to the solid surface [17]. The larger θ is, the poorer the wettability of the liquid phase to the solid surface is.

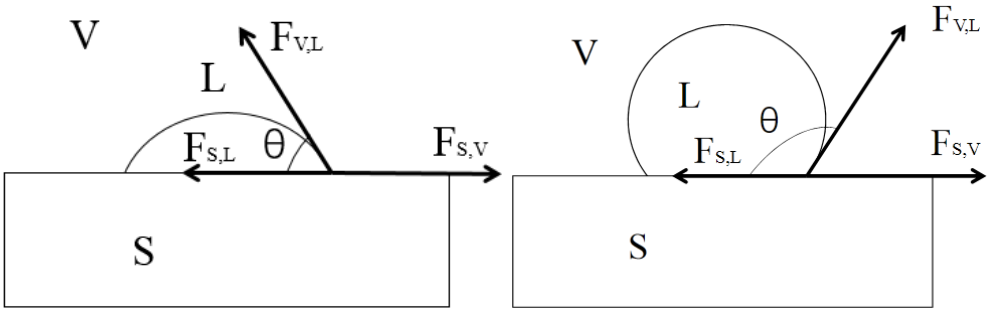

(a) θ<90° (b) θ>90°

Figure 8. Spheroidization effect process

The spheroidization effect leads to the formation of uneven surface, resulting in uneven thickness of the next layer of powder. Meanwhile, as the powder melts and solidifies, the solid volume shrinks [18], causing the uneven thickness of the next powder layer which is larger than the theoretical powder thickness. Part of the underlying powder is difficult to completely melt under the condition that the melting pool has a limited melting width and depth, and the un-melted area is exposed after being polished, which is shown as irregularly shaped and large-sized keyhole pores. As shown in Figure 10, there is un-melted powder in the keyhole. Since the melting path is in a straight line and the "valleys" between the adjacent melting paths are approximately parallel to each other, the keyhole pores are nearly parallel and linearly distributed, as shown in figure 9.

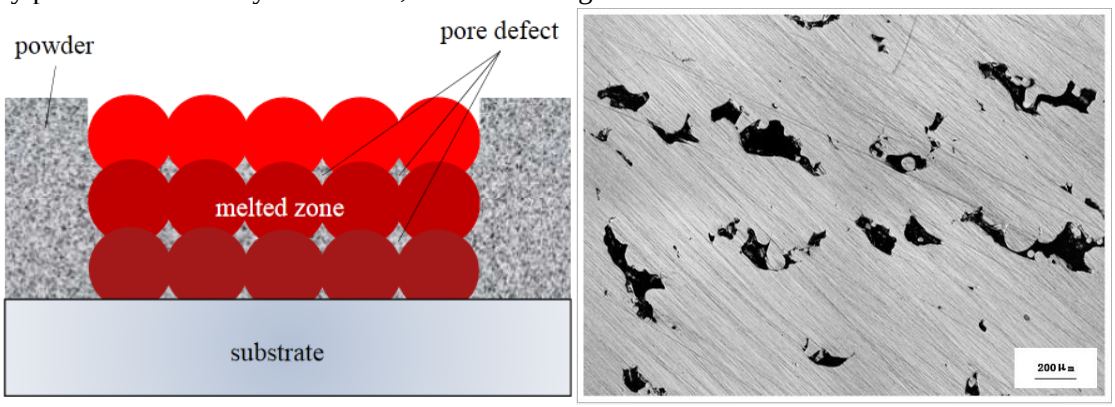

(a) Keyhole pores formation process diagram (b) Keyhole pores distributed morphology

Figure 9. Irregular keyhole pores formation process

3.3.2. Gas hole pore defect formation mechanism analysis

Before forming SLM cobalt-chromium alloy, the forming chamber was repeatedly filled with nitrogen twice to ensure that the oxygen content of forming chamber was less than 0.2%. Due to the gap among the cobalt-chromium alloy powder filled with nitrogen, when the high-energy density laser beam irradiates the powder bed, the powder rapidly absorbs heat and melts, and the cobalt-chromium alloy doesn't chemically react with nitrogen, thereby causing the nitrogen in the molten pool to be forced outward. However, due to rapid solidification of molten pool, nitrogen bubbles can't be discharged in time to form round pores, as seen in figure 7. Meanwhile, some components of cobalt-chromium alloy powder whose boiling point is lower vaporize at the high temperature, so the vaporized gas generated in the internal of molten pool also can't be discharged in time to form round pores. These stomatal defects are approximately circular, smaller in size, distributed between a few microns and tens of nanometers, as shown in Figure 7. Formation process of micro round stomatal pore defect is shown in Figure 11.

In summary, we divided the pore defect into two categories. One is the larger sized and irregular shaped keyhole pores, which is caused by parts of the underlying powder unmolten due to

spheroidization effect and volume shrinkage of powder melting and solidifying. The other is micro round gas pore defects which is formed due to the molten pool solidifying too fast, causing that the internal nitrogen and vaporized gases of some low-boiling components can't be timely discharged.

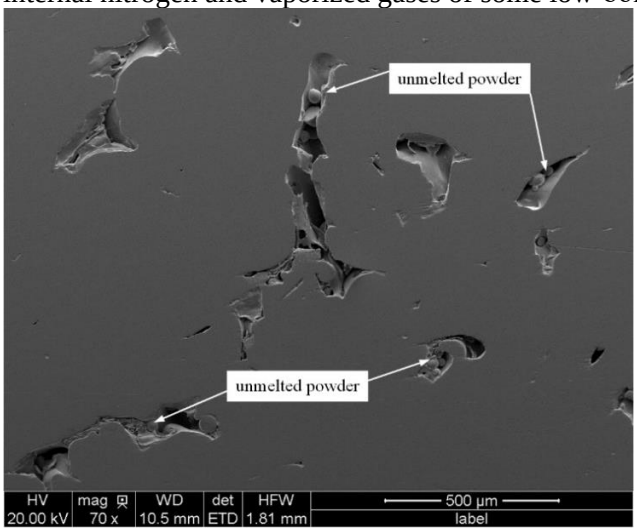

Figure 10. SEM image of keyhole pores morphology

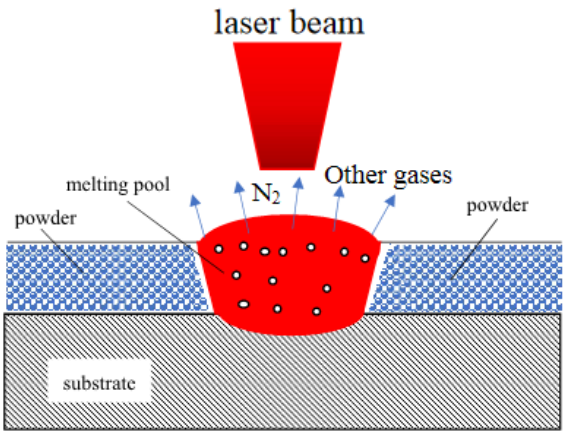

Figure 11. Gas hole pore defect formation process diagram

3.4. Method of controlling pore defect

Based on the analysis of formation mechanism of pore defect, two different types of pores are proposed, as follows are methods to reduce the porosity:

- Select the appropriate process parameters, especially the laser power, scanning speed, powder thickness, scanning distance to inhibit the spheroidization effect to ensure that the powder thickness of each layer is nearly uniform during SLM forming process; Adopt the method of powder thickness compensation to reduce the volume shrinking effect caused by the powder melting and solidifying, so that each layer of powder can be completely melted. Figure 12a and b, respectively, are the internal pore defect topography of the thickness of 0.07mm and 0.03mm. Therefore, the method of reducing the powder thickness can be used to suppress the occurrence of large-size keyhole pore defect.

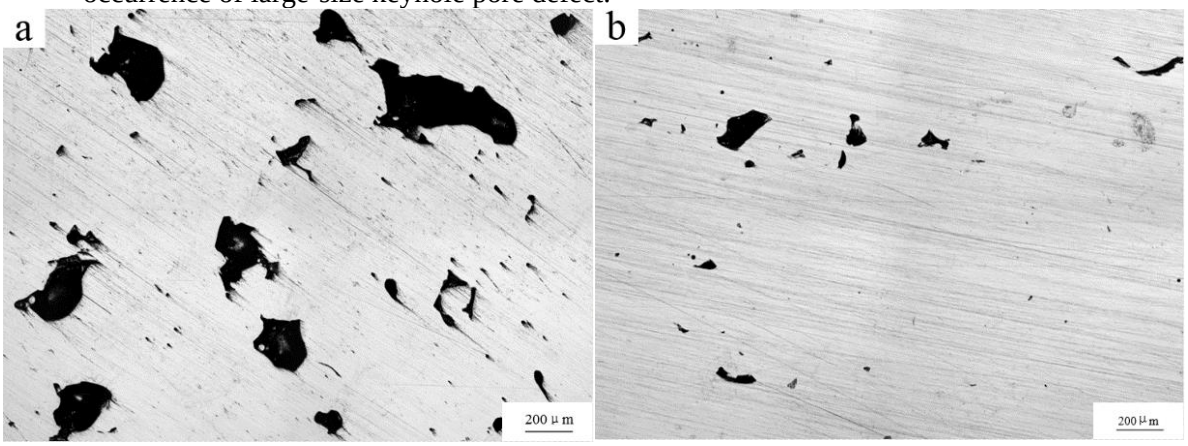

Figure 12. Internal keyhole pore defect morphology under the conditions of powder thickness of a = 0.07 and b = 0.03

- Try to use small size cobalt-chromium alloy powder of good sphericity. Because the bulk density of these powders is high, effectively reducing the gap among the powders and thus

reducing the filling of nitrogen, ultimately reducing the gas pore defects due to nitrogen emissions during the forming process.

- Pre-heating the substrate and powder prior to forming the SLM parts can reduce the temperature gradient to lower the cooling rate of the molten pool and allow more time for the gas to discharge to inhibit the occurrence of gas hole pore defect. Fig. 13a and Fig. 3b show the internal gas pore defect distribution of cobalt-chromium alloy SLM formed parts (some of which are indicated by arrows) when the substrate temperature is 20°C and 200°C, respectively. The amount of gas hole in Fig. 13a is obviously more than that in Fig. 13b.

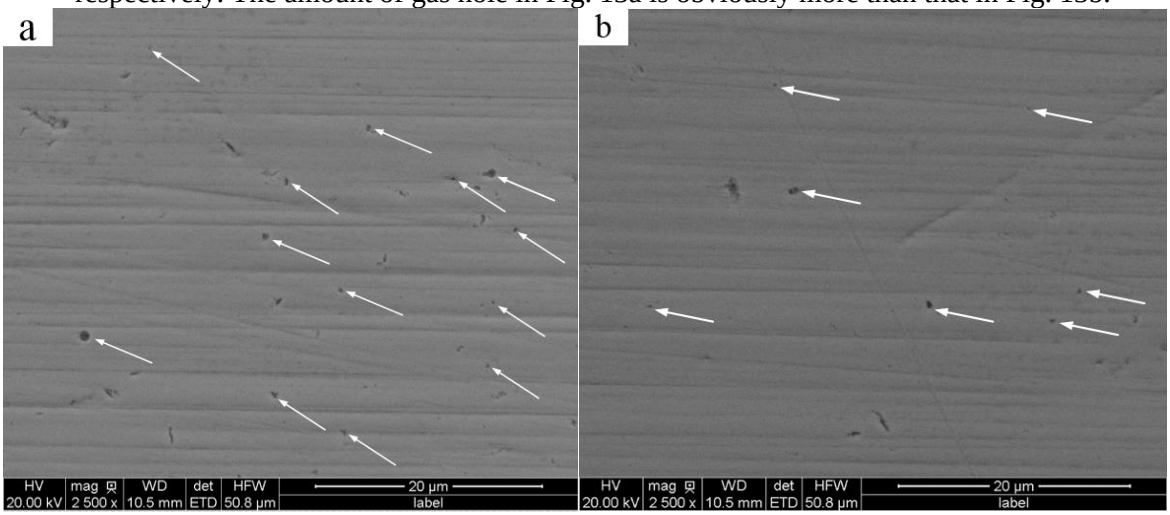

Figure 13. Gas hole pore defect morphology under the conditions at the temperature of a = 20 °C and b = 200 °C

4. Conclusion

- The influence extent of process parameters on the density of SLM formed parts is as follows: powder thickness > laser power> scanning distance> scanning speed. Powder thickness is the most important factor affecting the density of the parts. In the process parameters of P = 170W, v = 500mm / s, h = 0.03mm, d = 0.08mm, the highest density of the forming part is up to 97.05%.
- The amount and size of the pore defect are the direct factors that affect the density of the SLM formed part. The density is larger while the amount and size of the pores are smaller. The pore defect are divided into two categories. One is the larger sized and irregular shaped keyhole pore defect, which is caused by parts of the underlying powder unmolten due to spheroidization effect and volume shrinkage of powder melting and solidifying. The other is micro round gas hole pore defect which is formed due to the molten pool solidifying too fast, causing that the internal nitrogen and vaporized gases of some low-boiling components can't be timely discharged.
- Select the appropriate process parameters and inhibit the spheroidization effect and the powder melting and solidifying volume shrinkage effect. The powder can be completely melted by reducing the powder thickness to inhibit the occurrence of keyhole pore defect. To use small-sized cobalt-chromium alloy powder of good sphericity can effectively reduce the gap among the powders and thus reduce the filling of nitrogen, ultimately reduce the gas hole pore defect due to nitrogen emissions during the forming process. Pre-heating the substrate and powder prior to forming the SLM parts can reduce the temperature gradient to lower the cooling rate of the molten pool and allow more time for the gas to discharge to inhibit the occurrence of gas pore defect.

References

[1] Over C, Meiners W, Wissenbach K, Hutfless J and Lindemann M 2001 Selective laser melting: a new approach for the direct manufacturing of metal parts and tools *Frankfurt:1st International Conference on laser assisted Net Shape Engineering*
[2] Kruth J, Mercelis P, Vaerenbergh J, Froyen L and Rombouts M 2005 Binding mechanisms in selective laser sintering and melting *Rapid Prototyping Journal* **11** 26–36
[3] Yue B, Varadarajan K, Ai S, Rubash H, Tang T and Li G 2011 Differences of knee anthropometry between Chinese and white men and women *The Journal of Arthroplasty* **26** 124–30
[4] Mahfouz M, Fatah E, Bowers L and Scuderi G 2012 Three-dimensional morphology of the knee reveals ethnic differences *Clinical Orthopaedics and Related Research* **470** 172–185.
[5] Xiang N, Xin X, Chen J and Wei B 2012 Metal-ceramic bond strength of Co-Cr alloy fabricated by selective laser melting *Journal of Dentistry* **40** 453–57
[6] Zhang B, Huang Q, Gao Y, Luo P and Zhao C 2012 Preliminary study on some properties of Co-Cr dental alloy formed by selective laser melting technique *Journal of Wuhan University of Technology-Mater* **27** 665–68
[7] Oh K, Kang D, Choi G and Kim K 2007 Cytocompatibility and electrochemical properties of Ti-Au alloys for biomedical applications *Journal of Biomedical Materials Research Part B: Applied Biomaterials* **83** 320–26
[8] Yu Z, Zheng Y, Zhou L, Wang B, Niu J, Huang F and Zhang Y 2008 Shape memory effect and superelastic property of a novel Ti-3Zr-2Sn-3Mo-15Nb alloy *Rare Metal Materials and Engineering* **37** 1–5
[9] Qian D, Chen C, Zhang M, Wang X and Jing H 2016 Study on microstructure and micro-mechanical properties of porous aluminum alloy fabricated by selective laser melting *Chinese Journal of Lasers* **43** 66–73
[10] Zhao J, Qiu Y, Liu F and Chen J 2014 Research of surface roughness and relative density of SLM medical Co-Cr alloy *Applied Laser* **34** 524–27
[11] Santos E, Osakada K, Shiomi M, Kitamura Y and Abe F 2004 Microstructure and mechanical properties of pure titanium models fabricated by selective laser melting *Mechanical Engineering Science* **218** 711–19
[12] Lu Y, Wu S, Gan Y, Li J, Zhao C, Zhuo D and Lin J 2015 Investigation on the microstructure, mechanical property and corrosion behavior of the selective laser melted CoCrW alloy for dental application *Materials Science and Engineering C* **49** 517–25
[13] Aboulkhair N, Everitt N, Ashcroft I and Tuck C 2014 Reducing porosity in AlSi10Mg parts processed by selective laser melting *Additive Manufacturing* **1**–**4** 77–86
[14] Monroy K, Delgado J and Ciurana J 2013 Study of the pore formation on CoCrMo alloys by selective laser melting manufacturing process *Procedia Engineering* **63** 361–69
[15] Gong H, Rafi K, Gu H, Starr T and Stucker B 2014 Analysis of defect generation in Ti–6Al–4V parts made using powder bedfusion additive manufacturing processes *Additive Manufacturing* **1**–**4** 87–98
[16] Dai D and Gu D 2015 Tailoring surface quality through mass and momentum transfer modeling using a volume of fluid method in selective laser melting of Tic/AlSi10Mg powder *International Journal of Machine Tools & Manufacture* **88** 95–107
[17] Du J 2014 Research on process experiment of selective laser melting with GH4169 nickel-based alloy powder Taiyuan: North University of China 34–35
[18] Huang Y 2016 Finite element analysis of thermal behavior of metal powder during selective laser melting under moving heat source Beijing: North China Electric Power University 30–34